

DOI: 10.7511/jslx20230314002

爆炸荷载线性强化抗力模型梁构件动力系数研究

耿少波^{1,2}, 韩晓丹¹, 牛艳伟^{*2}, 韩云山¹, 马林林¹

(1. 中北大学 环境与安全工程学院, 太原 030051;

2. 长安大学 公路大型结构安全教育部工程研究中心, 西安 710064)

摘要: 目前梁构件抗爆设计动力系数计算常采用理想弹塑性抗力模型, 制约着塑性强化抗力构件的精细化抗爆设计。为解决线性强化抗力类型梁构件的爆炸作用动力系数计算问题, 由抗力强化系数和阻尼比数值大小关系, 分三种情况推导了柔性和刚性两类构件关于延性比的动力系数解析解。有限元分析及规范对比算例表明, 本文推导理论公式精度较高, 与抗爆设计规范公式计算结果趋势相似; 延性比为1时, 抗力强化系数与动力系数无关; 延性比大于1且抗力强化系数小于0.01时, 可忽略抗力强化系数的影响; 延性比大于2时, 需考虑阻尼参数后完成抗爆设计分析; 延性比大于3时且抗力强化系数大于0.1时, 线性强化抗力模型具有较好经济效益。

关键词: 线性强化抗力模型; 爆炸荷载; 动力系数; 延性比; 梁构件

中图分类号: TH212; O302

文献标志码: A

文章编号: 1007-4708(2024)05-0886-08

1 引言

等效单自由度法 SDOF (Single Degree of Freedom) 作为一种直观简易的方法, 采用理想弹塑性抗力模型后, 广泛用于梁构件爆炸作用的试验对比^[1-4]和理论分析^[5-9]。为提高计算精度, 学者们不断完善 SDOF 计算方法, 如 Liu 等^[10]提出考虑钢筋混凝土 RC (Reinforced Concrete) 梁破损程度的 SDOF 方法; 陈万祥等^[11]完成混杂纤维轻骨料混凝土梁的爆炸作用试验后, 提出考虑面力效应的改进 SDOF 计算方法; Nagata 等^[12]提出修正爆炸荷载使得 SDOF 方法满足近场爆炸荷载下 RC 梁的振动响应; Chen 等^[13]的混合纤维增强混凝土梁爆炸试验、Yao 等^[14]的 RC 短梁构件、Wang 等^[15]的钢管混凝土梁构件和 Ritchie 等^[16]的方钢管梁构件爆炸试验均说明阻尼参数对 SDOF 方法响应有影响; 方秦等^[17]完成了构件端部阻尼、耿少波等^[18]完成了阻尼参数对爆炸作用 SDOF 方法下振动位移影响的定量分析。

很多学者认识到理想弹塑性抗力模型与抗爆构件实际抗力存在一定偏差。如蔡镇清等^[19]通过

LS-DYNA 分析了爆炸荷载作用下两端固支约束梁柱、板构件的抗力-位移曲线, 指出 RC 构件塑性阶段采用抗力强化模型较为准确; Nassr 等^[20]完成的工字型钢梁远场爆炸试验, 也表明采用线性强化抗力模型较为适宜; Bruhl 等^[21]的爆炸作用低合金钢梁试验, 梁在塑性阶段表现出抗力强化特征; Cui 等^[22]通过混凝土结构试验验证了塑性阶段存在抗力强化效应。

因此, 爆炸作用 SDOF 方法采用线性强化抗力模型后将更准确地描述爆炸荷载作用下梁构件的动力响应。理想弹塑性抗力模型忽略了抗力强化效应, 这对爆炸作用构件位移响应和抗爆设计动力系数参数影响如何, 目前学术界尚无定量结论。

本文区分刚性构件和柔性构件后, 建立含抗力强化参数的 SDOF 振动方程, 求解爆炸荷载作用下梁构件振动分析的位移、动力系数及延性比表达式, 通过算例验证本文理论解答合理性后, 讨论塑性强化抗力对动力系数的影响, 完成与理想弹塑性抗力模型下动力系数结果对比, 提出了抗爆设计合理建议。本文的 SDOF 方法参数全面、通用性强,

收稿日期: 2023-03-14; 修改稿收到日期: 2023-05-06.

基金项目: 国家自然科学基金(51408558); 山西省基础研究计划(202203021211099); 旧桥检测与加固技术交通运输行业重点实验室(长安大学)开放基金(300102212516); 陕西省自然科学基金基础研究计划(2023-JC-YB-292); 中央高校基本科研业务费专项资金(300102214907)资助项目。

作者简介: 牛艳伟* (1981-), 男, 博士, 副教授(E-mail: niuyanwei@chd.edu.cn).

引用本文: 耿少波, 韩晓丹, 牛艳伟, 等. 爆炸荷载线性强化抗力模型梁构件动力系数研究[J]. 计算力学学报, 2024, 41(5): 886-893.
GENG Shao-bo, HAN Xiao-dan, NIU Yan-wei, et al. Study on dynamic coefficient of beam members with linear hardening resistance model under blast load [J]. Chinese Journal of Computational Mechanics, 2024, 41(5): 886-893.

动力系数相关表达式更加准确,有利于抗爆防护工程精细化应用。

2 爆炸荷载柔性构件动力系数求解

2.1 爆炸荷载柔性梁构件定义

设 t_i 为爆炸荷载作用时长, t_T 为构件完成弹性振动准备进入塑性振动所需时长。若 $t_i < t_T$, 爆炸荷载作用时长内构件尚未完成弹性振动, 构件显示出柔性特征, 称此类梁构件为柔性梁构件。包含常规武器在内的化学爆炸荷载作用时间极短, 常认为柔性构件在爆炸荷载作用消失后构件振动达到最大弹塑性位移的时间 $t_m > t_T$ [22], 即柔性构件时间参数为 $t_i < t_T < t_m$ 。

爆炸荷载作用下梁构件等效 SDOF 方法如图 1(a)所示, 采用线性强化抗力模型动力响应的抗力与变形关系如图 1(b)所示。

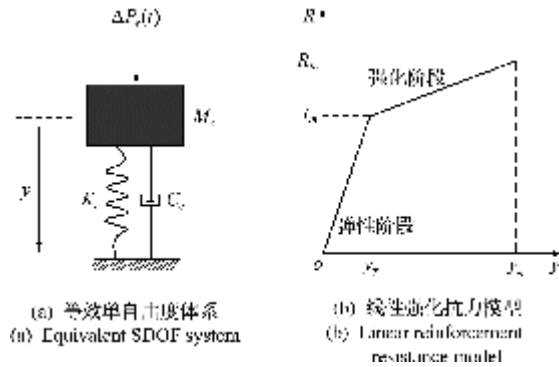


图 1 考虑线性强化抗力等效单自由度体系
Fig. 1 Equivalent single degree of freedom system with linear hardening resistance

2.2 弹性阶段强迫振动

此时对应时长为 $0 < t < t_i$, 等效 SDOF 的弹性阶段强迫振动方程表示为

$$M_e \ddot{y} + C_e \dot{y} + K_e y = \Delta P_e(t) \quad (1)$$

式中 M_e 为弹性阶段等效质量, C_e 为弹性阶段等效阻尼, K_e 为弹性阶段等效刚度, y 为构件的振动位移, $\Delta P_e(t)$ 为等效构件承受的等效爆炸荷载。各等效系数分别为

$$M_e = k_M m l, \quad C_e = 2\xi \sqrt{k_M m l k_L K}, \quad K_e = k_L K \quad (2)$$

式中 m 为构件单位长度质量, l 为构件跨长, ξ 为构件阻尼比, K 为构件刚度, k_M 为构件弹性阶段质量变换系数, k_L 为构件弹性阶段荷载变换系数。中国抗爆规范采用的爆炸荷载为 [21]

$$\Delta P_e(t) = \begin{cases} \Delta P_m l k_L (1 - t/t_i) & (0 \leq t \leq t_i) \\ 0 & (t > t_i) \end{cases} \quad (3)$$

求解方程(1)后将 t_i 代入解析式, 可得构件

弹性强迫振动阶段末的位移和速度表达式为

$$y_i = y_{st} \left\{ e^{-\xi \omega t_i} \left[-\left(1 + \frac{2\xi}{\omega t_i}\right) \cos \omega_d t_i + \left[\frac{1}{\omega_d t_i} - \frac{\xi \omega}{\omega_d} \left(1 + \frac{2\xi}{\omega t_i}\right) \right] \sin \omega_d t_i \right] + \frac{2\xi}{\omega t_i} \right\} \quad (4)$$

$$v_i = y_{st} \left\{ e^{-\xi \omega t_i} \left[\left[\left(1 + \frac{2\xi}{\omega t_i}\right) \left(\frac{\xi^2 \omega^2}{\omega_d} + \omega_d \right) - \frac{\xi \omega}{\omega_d t_i} \right] \times \sin \omega_d t_i + \frac{\cos \omega_d t_i}{t_i} \right] - \frac{1}{t_i} \right\} \quad (5)$$

式中 ω 为构件无阻尼振动频率, ω_d 为构件含阻尼振动频率, y_{st} 为将动载 ΔP_m 作为静载时构件位移, 各参数计算公式为

$$\omega = \sqrt{K_e/M_e}, \quad \omega_d = \omega \sqrt{1 - \xi^2}, \quad y_{st} = \Delta p_m l / K \quad (6)$$

2.3 弹性阶段自由振动

爆炸荷载作用结束后, 构件开始做以 y_i 和 v_i 为初始条件的弹性自由振动, 即 $t_i < t < t_T$ 时, 等效 SDOF 弹性阶段自由振动的方程为

$$M_e \ddot{y} + C_e \dot{y} + K_e y = 0 \quad (7)$$

求解方程(7)后将 t_T 代入解析式, 可得构件弹性自由振动阶段结束时构件的位移和速度表达式为

$$y_T = e^{-\xi \omega (t_T - t_i)} \left[y_i \cos(\omega_d t_T - \omega_d t_i) + \frac{v_i + \xi \omega y_i}{\omega_d} \times \sin(\omega_d t_T - \omega_d t_i) \right] \quad (8)$$

$$v_T = e^{-\xi \omega (t_T - t_i)} \left[v_i \cos(\omega_d t_T - \omega_d t_i) - \left(\omega_d y_i + \frac{\xi \omega v_i + \xi^2 \omega^2 y_i}{\omega_d} \right) \sin(\omega_d t_T - \omega_d t_i) \right] \quad (9)$$

2.4 塑性阶段自由振动

当 $t > t_T$, 构件开始做以 y_T 和 v_T 为初始条件的塑性自由振动, 即 $t_T < t < t_m$ 时, 考虑塑性抗力强化效应后的等效 SDOF 方程为

$$m_e \ddot{y} + c_e \dot{y} + \alpha K_e y + (1 - \alpha) K_e y_T = 0 \quad (10)$$

式中 m_e 为塑性阶段等效质量, c_e 为塑性阶段等效阻尼, α 为构件塑性阶段与弹性阶段等效刚度的比值, 称为抗力强化系数, αK_e 为塑性阶段等效刚度。令 k_m 为塑性阶段质量变换系数, k_l 为塑性阶段荷载变换系数, 则 m_e 和 c_e 计算公式为

$$m_e = k_m m l, \quad c_e = 2\xi \sqrt{k_m m l k_L K} \quad (11)$$

根据阻尼比 ξ 和抗力强化系数 α 的数值关系, 方程(10)的求解需分以下三种情况。

(1) $\xi^2 = \alpha$ 时方程(10)求解。此时, 塑性自由振动的位移及速度表达式求解如下

$$y = [D_1 + D_2(t - t_T)] e^{-\sqrt{k_M - l/k_m - l} \xi \omega (t - t_T)} + [(\alpha - 1) y_T] / \alpha \quad (12)$$

$$v = e^{-\sqrt{k_{M-L}/k_{m-l}} \xi \omega (t-t_T)} \left\{ D_2 - \sqrt{k_{M-L}/k_{m-l}} \times \xi \omega [D_1 + D_2 (t-t_T)] \right\} \quad (13)$$

式中 k_{M-L} 和 k_{m-l} 分别为弹性阶段和塑性阶段质量变换系数与荷载变换系数比值。将式(8,9)代入式(12,13)后解得 D_1 和 D_2 的表达式为

$$D_1 = \frac{y_T}{\alpha}, D_2 = v_T + \xi \omega \frac{y_T}{\alpha} \sqrt{\frac{k_{M-L}}{k_{m-l}}} \quad (14)$$

令式(13)为0,可得梁构件达到振动最大位移 y_m 时对应的时刻 t_m 为

$$t_m = \left[\sqrt{\frac{k_{M-L}}{k_{m-l}}} \left(\xi \omega + \frac{\xi^2 \omega^2 y_T}{\alpha v_T} \sqrt{\frac{k_{M-L}}{k_{m-l}}} \right) \right]^{-1} + t_T \quad (15)$$

将式(14,15)代入式(12),得到构件振动的最大位移 y_m 。

根据爆炸荷载梁构件弹塑性变形理论和抗爆参数定义可知,等效静载动力系数 k_h 和延性比 β 的表达式为^[22]

$$k_h = y_T / y_{st}, \beta = y_m / y_T \quad (16)$$

(2) $\xi^2 < \alpha$ 时方程(10)求解。此时位移和速度解为

$$y = e^{-\sqrt{k_{M-L}/k_{m-l}} \xi \omega (t-t_T)} \times \left\{ D_3 \cos \left[\sqrt{(\alpha - \xi^2)} (k_{M-L}/k_{m-l}) \omega (t-t_T) \right] + D_4 \sin \left[\sqrt{(\alpha - \xi^2)} (k_{M-L}/k_{m-l}) \omega (t-t_T) \right] + (\alpha - 1) / \alpha y_T \right\} \quad (17)$$

$$v = \sqrt{k_{M-L}/k_{m-l}} \omega e^{-\sqrt{k_{M-L}/k_{m-l}} \xi \omega (t-t_T)} \times \left\{ (D_4 \sqrt{\alpha - \xi^2} - D_3 \xi) \times \cos \left[\sqrt{(\alpha - \xi^2)} (k_{M-L}/k_{m-l}) \omega (t-t_T) \right] - (D_3 \sqrt{\alpha - \xi^2} + D_4 \xi) \times \sin \left[\sqrt{(\alpha - \xi^2)} (k_{M-L}/k_{m-l}) \omega (t-t_T) \right] \right\} \quad (18)$$

同理,可解得 D_3 和 D_4 的表达式为

$$D_3 = \frac{y_T}{\alpha}, D_4 = \sqrt{\frac{k_{m-l}}{k_{M-L}}} \frac{v_T}{\omega \sqrt{\alpha - \xi^2}} + \frac{y_T \xi}{\alpha \sqrt{\alpha - \xi^2}} \quad (19)$$

且可知构件达到正向振动最大位移 y_m 时对应的时刻 t_m 为

$$t_m = \sqrt{\frac{k_{m-l}}{k_{M-L}}} \frac{1}{\omega \sqrt{\alpha - \xi^2}} \arctan \left(\frac{\sqrt{\alpha - \xi^2} D_4 - \xi D_3}{\sqrt{\alpha - \xi^2} D_3 + \xi D_4} \right) + t_T \quad (20)$$

将式(20,19)代入式(17),得到构件振动的最大位移 y_m 。

(3) $\xi^2 > \alpha$ 时方程(10)求解。此时位移和速度解为

$$y = \left[D_5 e^{-\omega \sqrt{k_{M-L}/k_{m-l}} (\xi - \sqrt{\xi^2 - \alpha}) (t-t_T)} + D_6 e^{-\omega \sqrt{k_{M-L}/k_{m-l}} (\xi + \sqrt{\xi^2 - \alpha}) (t-t_T)} \right] + (\alpha - 1) y_T / \alpha \quad (21)$$

$$v = -\omega \sqrt{k_{M-L}/k_{m-l}} \left[(\xi - \sqrt{\xi^2 - \alpha}) D_5 \times e^{-\omega \sqrt{k_{M-L}/k_{m-l}} (\xi - \sqrt{\xi^2 - \alpha}) (t-t_T)} + (\xi + \sqrt{\xi^2 - \alpha}) D_6 \times e^{-\omega \sqrt{k_{M-L}/k_{m-l}} (\xi + \sqrt{\xi^2 - \alpha}) (t-t_T)} \right] \quad (22)$$

同理,可解得 D_5 和 D_6 的表达式为

$$D_5 = \frac{\sqrt{k_{m-l}/k_{M-L}}}{2\sqrt{\xi^2 - \alpha}} \left[\frac{v_T}{\omega} + \sqrt{\frac{k_{M-L}}{k_{m-l}}} (\xi + \sqrt{\xi^2 - \alpha}) \frac{y_T}{\alpha} \right] \quad (23)$$

$$D_6 = y_T / \alpha - D_5$$

且可得构件达到正向振动最大位移 y_m 时对应的时刻 t_m 为

$$t_m = \frac{1}{2\omega \sqrt{\xi^2 - \alpha}} \sqrt{\frac{k_{m-l}}{k_{M-L}}} \ln \frac{(\sqrt{\xi^2 - \alpha} + \xi) D_6}{(\sqrt{\xi^2 - \alpha} - \xi) D_5} + t_T \quad (24)$$

同理可得此时的最大位移 y_m 。分别将上述三种 y_m 解代入式(16),即可得到各自对应的延性比解析式。结合式(8,16)可得柔性构件动力系数 k_h 表达式。

3 爆炸荷载刚性构件动力系数求解

3.1 爆炸荷载刚性梁构件定义

类似于2.1节中相关参数定义,刚性梁构件指的是完成弹性振动的时间 t_T 小于爆炸荷载作用的时间 t_i , 此类梁构件的时间参数为 $t_T < t_i < t_m$ 。

3.2 弹性阶段强迫振动

此时对应时长为 $0 < t < t_T$, 类似于2.2节求解,求解方程(1)后将 t_T 代入解析式,可求解出构件弹性强迫振动阶段结束时的位移 y_T 和速度 v_T , 且可得到刚性构件动力系数 k_h 表达式。

3.3 塑性阶段强迫振动

构件从弹性振动进入塑性振动后,爆炸荷载尚未消失,即当 $t_T < t < t_i$ 时,等效 SDOF 的塑性阶段强迫振动方程可表示为

$$m_e \ddot{y} + c_e \dot{y} + \alpha K_e y + (1 - \alpha) K_e y_T = \frac{t_i - t}{t_i} \Delta P_m l k_L \quad (25)$$

类似于2.4节中柔性构件求法,方程(25)也需分三种情况进行求解。

(1) $\xi^2 = \alpha$ 时方程(25)求解。此时,塑性强迫振动的位移和速度可表示为

$$y = \left\{ [D_7 + D_8(t-t_T)] e^{-\sqrt{k_{M-L}/k_{m-l}} \xi \omega(t-t_T)} - \frac{y_{st}}{\alpha t_i} (t-t_T) + y_T + \frac{y_{st}(t_i-t_T) - y_T t_i}{\alpha t_i} + \frac{2y_{st}\xi}{\alpha^2 \theta_i} \right\} \quad (26)$$

$$v = \left\{ D_8 - \sqrt{\frac{k_{M-L}}{k_{m-l}}} \xi \omega [D_7 + D_8(t-t_T)] \right\} \times e^{-\sqrt{k_{M-L}/k_{m-l}} \xi \omega(t-t_T)} - \frac{y_{st}}{\alpha t_i} \quad (27)$$

式中 $\theta_i = \omega t_i$ 。将初始位移 y_T 和速度 v_T 代入式(26,27)后,可得 D_7 和 D_8 的表达式为

$$D_7 = \frac{y_T t_i - y_{st}(t_i - t_T)}{\alpha t_i} - \frac{2y_{st}\xi}{\alpha^2 \theta_i}$$

$$D_8 = v_T + \sqrt{\frac{k_{M-L}}{k_{m-l}}} \xi \omega D_7 + \frac{y_{st}}{\alpha t_i} \quad (28)$$

(2) $\xi^2 < \alpha$ 时方程(25)求解。此时位移和速度解为

$$y = e^{-\sqrt{k_{M-L}/k_{m-l}} \xi \omega(t-t_T)} \times \left\{ D_9 \cos \left[\sqrt{(\alpha - \xi^2)(k_{M-L}/k_{m-l})} \omega(t-t_T) \right] + D_{10} \sin \left[\sqrt{(\alpha - \xi^2)(k_{M-L}/k_{m-l})} \omega(t-t_T) \right] \right\} - \frac{y_{st}}{\alpha t_i} (t-t_T) + y_T + \frac{y_{st}(t_i-t_T) - y_T t_i}{\alpha t_i} + \frac{2y_{st}\xi}{\alpha^2 \theta_i} \quad (29)$$

$$v = \omega \sqrt{k_{M-L}/k_{m-l}} e^{-\sqrt{k_{M-L}/k_{m-l}} \xi \omega(t-t_T)} \times \left\{ -(D_9 \sqrt{\alpha - \xi^2} + D_{10} \xi) \times \sin \left[\sqrt{(\alpha - \xi^2)(k_{M-L}/k_{m-l})} \omega(t-t_T) \right] + (D_{10} \sqrt{\alpha - \xi^2} - D_9 \xi) \times \cos \left[\sqrt{(\alpha - \xi^2)(k_{M-L}/k_{m-l})} \omega(t-t_T) \right] \right\} - \frac{y_{st}}{\alpha t_i} \quad (30)$$

同理可得 D_9 和 D_{10} 表达式为

$$D_9 = \frac{y_{st}(t_i - t_T) - y_T t_i}{\alpha t_i} - \frac{2y_{st}\xi}{\alpha^2 \theta_i}$$

$$D_{10} = \frac{v_T}{\omega \sqrt{(\alpha - \xi^2)k_{M-L}}} + \frac{y_{st}}{\alpha \theta_i \sqrt{(\alpha - \xi^2)}} \sqrt{\frac{k_{m-l}}{k_{M-L}}} + \frac{\xi D_9}{\sqrt{\alpha - \xi^2}} \quad (31)$$

(3) $\xi^2 > \alpha$ 时方程(25)求解。此时位移和速度解为

$$y = D_{11} e^{-\omega \sqrt{k_{M-L}/k_{m-l}} (\xi - \sqrt{\xi^2 - \alpha})(t-t_T)} + D_{12} e^{-\omega \sqrt{k_{M-L}/k_{m-l}} (\xi + \sqrt{\xi^2 - \alpha})(t-t_T)} + y_T + \frac{y_{st}(t_i - t_T) - y_T t_i}{\alpha t_i} + \frac{2\xi y_{st}}{\alpha^2 \theta_i} - \frac{y_{st}}{\alpha t_i} (t-t_T) \quad (32)$$

$$v = -\omega \sqrt{k_{M-L}/k_{m-l}} (\xi - \sqrt{\xi^2 - \alpha}) \times D_{11} e^{-\omega \sqrt{k_{M-L}/k_{m-l}} (\xi - \sqrt{\xi^2 - \alpha})(t-t_T)} - \omega \sqrt{k_{M-L}/k_{m-l}} (\xi + \sqrt{\xi^2 - \alpha}) \times D_{12} e^{-\omega \sqrt{k_{M-L}/k_{m-l}} (\xi + \sqrt{\xi^2 - \alpha})(t-t_T)} - \frac{y_{st}}{\alpha t_i} \quad (33)$$

同理,可解得 D_{11} 和 D_{12} 表达式为

$$D_{11} = \sqrt{k_{m-l}/k_{M-L}} \frac{v_T}{2\omega \sqrt{\xi^2 - \alpha}} + \frac{y_{st}}{2\alpha \theta_i \sqrt{\xi^2 - \alpha}} + \frac{(\xi + \sqrt{\xi^2 - \alpha}) [\alpha \theta_i y_T - \alpha \omega y_{st}(t_i - t_T) - 2\xi y_{st}]}{2\alpha^2 \theta_i \sqrt{\xi^2 - \alpha}}$$

$$D_{12} = \frac{y_T t_i - y_{st}(t_i - t_T)}{\alpha t_i} - \frac{2\xi y_{st}}{\alpha^2 \theta_i} - D_{11} \quad (34)$$

将 $t = t_i$ 分别代入上述三种相关表达式,即可得到爆炸荷载作用结束时各自对应的 y_i 和 v_i 。

3.4 塑性阶段自由振动

当 $t > t_i$, 构件做以 y_i 和 v_i 为初始条件的塑性阶段自由振动,即 $t_i < t < t_m$ 时,考虑塑性阶段强化效应的等效 SDOF 方程与柔性构件相同。

此时方程也需要分以下三种情况进行求解。

(1) $\xi^2 = \alpha$ 时方程求解。此时,塑性自由振动的位移和速度表达式为

$$y = [D_{13} + D_{14}(t-t_i)] e^{-\sqrt{k_{M-L}/k_{m-l}} \xi \omega(t-t_i)} + (\alpha - 1) y_T / \alpha \quad (35)$$

$$v = e^{-\sqrt{k_{M-L}/k_{m-l}} \xi \omega(t-t_i)} \left\{ D_{14} - \sqrt{k_{M-L}/k_{m-l}} \xi \omega \times [D_{13} + D_{14}(t-t_i)] \right\} \quad (36)$$

将初始条件 y_i 和 v_i 代入式(35,36)后,解得 D_{13} 和 D_{14} 表达式为

$$D_{13} = y_i + (1 - \alpha) y_T / \alpha$$

$$D_{14} = v_i + \sqrt{k_{M-L}/k_{m-l}} \xi \omega D_{13} \quad (37)$$

令式(36)为 0,可得构件达到振动的最大位移 y_m 时对应的时刻 t_m 为

$$t_m = \frac{1}{\xi \omega \sqrt{k_{M-L}}} - [\alpha y_i + (1 - \alpha) y_T] / \left\{ \alpha v_i + \sqrt{\frac{k_{m-l}}{k_{M-L}}} \xi \omega [\alpha y_i + (1 - \alpha) y_T] \right\} + t_i \quad (38)$$

(2) $\xi^2 < \alpha$ 时方程求解。此时位移和速度解为

$$y = e^{-\sqrt{k_{M-L}/k_{m-l}} \xi \omega(t-t_i)} \times \left\{ D_{15} \cos \left[\sqrt{(\alpha - \xi^2)(k_{M-L}/k_{m-l})} (\omega t - \theta_i) \right] + D_{16} \sin \left[\sqrt{(\alpha - \xi^2)(k_{M-L}/k_{m-l})} (\omega t - \theta_i) \right] \right\} + [(\alpha - 1) / \alpha] y_T \quad (39)$$

$$v = \omega \sqrt{k_{M-L}/k_{m-l}} e^{-\sqrt{k_{M-L}/k_{m-l}} \xi \omega (t-t_i)} \times \left\{ (D_{16} \sqrt{\alpha - \xi^2} - D_{15} \xi) \times \cos[\sqrt{(\alpha - \xi^2)(k_{M-L}/k_{m-l})}(\omega t - \theta_i)] - (D_{15} \sqrt{\alpha - \xi^2} + D_{16} \xi) \times \sin[\sqrt{(\alpha - \xi^2)(k_{M-L}/k_{m-l})}(\omega t - \theta_i)] \right\} \quad (40)$$

同理,解得 D_{15}, D_{16} 表达式和 t_m 的解为

$$D_{15} = y_i + (1 - \alpha) y_T / \alpha \quad (41)$$

$$D_{16} = \frac{v_i}{\omega \sqrt{(\alpha - \xi^2) k_{M-L}}} + \frac{\alpha \xi y_i + (1 - \alpha) y_T \xi}{\alpha \sqrt{\alpha - \xi^2}} \quad (42)$$

$$t_m = \frac{1}{\omega \sqrt{(\alpha - \xi^2) k_{M-L}}} \arctan \frac{D_{16} \sqrt{\alpha - \xi^2} - D_{15} \xi}{D_{15} \sqrt{\alpha - \xi^2} + D_{16} \xi} + t_i \quad (43)$$

(3) $\xi^2 > \alpha$ 时方程求解。此时位移和速度解为

$$y = D_{17} e^{-\omega \sqrt{k_{M-L}/k_{m-l}} (\xi - \sqrt{\xi^2 - \alpha})(t-t_i)} + D_{18} e^{-\omega \sqrt{k_{M-L}/k_{m-l}} (\xi + \sqrt{\xi^2 - \alpha})(t-t_i)} + \frac{\alpha - 1}{\alpha} y_T \quad (44)$$

$$v = -\omega \sqrt{k_{M-L}/k_{m-l}} \left[(\xi - \sqrt{\xi^2 - \alpha}) \times D_{17} e^{-\omega \sqrt{k_{M-L}/k_{m-l}} (\xi - \sqrt{\xi^2 - \alpha})(t-t_i)} + (\xi + \sqrt{\xi^2 - \alpha}) D_{18} e^{-\omega \sqrt{k_{M-L}/k_{m-l}} (\xi + \sqrt{\xi^2 - \alpha})(t-t_i)} \right] \quad (45)$$

同理,可解得 D_{17} 和 D_{18} 表达式为

$$D_{17} = \frac{\sqrt{\frac{k_{m-l}}{k_{M-L}} \frac{v_i}{\omega} + (\xi + \sqrt{\xi^2 - \alpha}) (y_i + \frac{1-\alpha}{\alpha} y_T)}}{2 \sqrt{\xi^2 - \alpha}}$$

$$D_{18} = y_i + \frac{1-\alpha}{\alpha} y_T + D_{17} \quad (46)$$

且可得

$$t_m = \frac{1}{2 \omega \sqrt{\xi^2 - \alpha}} \sqrt{\frac{k_{m-l}}{k_{M-L}}} \ln \frac{(\sqrt{\xi^2 - \alpha} + \xi) D_{18}}{(\sqrt{\xi^2 - \alpha} - \xi) D_{17}} + t_i \quad (47)$$

分别将上述三种情况下的 t_m 表达式代入各自的位移表达式中即可得到相应的最大位移 y_m 。类似于 2.4 节的求法,同理可得对应的动力系数 k_h 和延性比 β 表达式。

4 本文理论验证

4.1 数值验证

为完成本文理论的数值验证,开展了爆炸作用下方钢管 LS-DYNA 有限元分析,构件长 1300 mm,截面为 60 mm×60 mm×3.75 mm,炸药当量 5 kg,矩形装药,爆距 2000 mm,空气和炸药采用 ALE 算法,方钢管采用 LAGRANGE 算法。空气域单元

尺寸 6 mm~7 mm,空气 287135 个单元,炸药 286 个单元,方钢管采用网格尺寸 5 mm 的壳单元,共 8290 个单元,两端固支边界条件,超压峰值荷载为 $\Delta P_m = 684$ kPa。当阻尼比 $\xi = 0.1$ 且抗力强化系数 $\alpha = 0.001$ 时,方钢管背爆面跨中挠度时程曲线分布如图 2 所示。

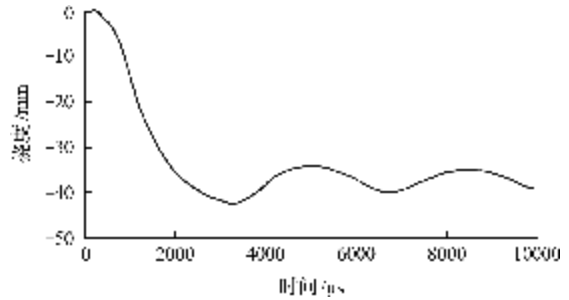


图 2 方钢管背爆面跨中典型位移时程曲线

Fig. 2 Typical displacement curve of mid span for square steel tube back to blast load

由数据可知,方钢管构件最大弹塑性位移为 42.3 mm,残余变形为 37.2 mm,最大弹性位移为 5.1 mm,延性比 β 为 8.294,动力系数 k_h 为 0.0342。

同理,利用本文理论完成了 $\alpha = 0.01 \sim 0.2$ 四种工况下动力系数理论计算及误差对比,列入表 1。

表 1 典型有限元工况误差分析

Tab. 1 Error analysis of typical finite element calculation cases

α	理论值 k_h	有限元值 k_h	误差/%
0.001	0.0321	0.0342	-6.14
0.01	0.0316	0.0335	-5.67
0.05	0.0307	0.0330	-6.97
0.1	0.0292	0.0312	-6.41
0.2	0.0273	0.0301	-9.30

由表 1 可知,本文推导结论与数值模拟结果误差较小,各种强化系数工况下误差均在 10% 以内,平均误差约 6.90%;抗力强化系数为 0.2 时,误差最大,约 9.30%;抗力强化系数为 0.01 时,误差最小,为 5.67%。

4.2 规范验证

以中国现行抗爆设计规范采用的等效 SDOF 方法动力系数公式为基准,开展理论验证,规范公式为^[23]

$$k_h = \left[\frac{2}{\theta_i} \sqrt{2\beta - 1} + \frac{2\beta - 1}{2\beta(1 + 4/\theta_i)} \right]^{-1} \quad (48)$$

本文以简支梁构件为分析对象,柔性和刚性两类构件分类验算,延性比计算范围为 $\beta = 1.0 \sim 4.0$,结构-荷载参数计算范围为 $\theta_i = 0.0 \sim 2.2$, k_{M-L}/k_{m-l} 取值为 1.18^[24],阻尼比取值 $\xi = 0.1$ 。

为考察塑性强化抗力对动力系数的影响, α 采

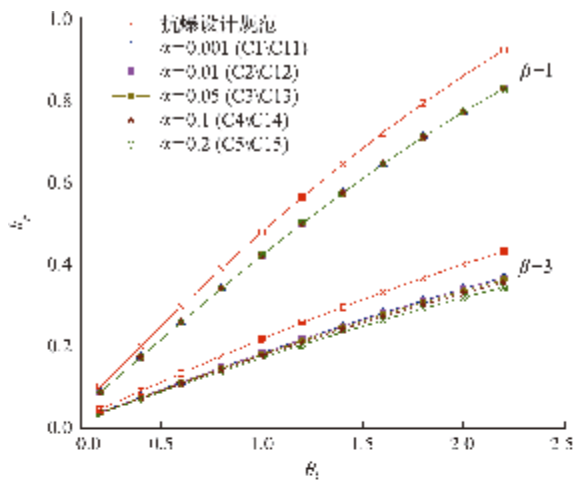
用 0.001(近似理想弹塑性/无强化)、0.01(接近无强化)、0.05(低度强化)、0.1(中低度强化)和 0.2(中高度强化)五种典型参数数值来表征,共计 20 种算例工况,列入表 2。各工况值及规范公式的对比如图 3 所示,相对误差如图 4 所示。

表 2 典型算例工况遴选

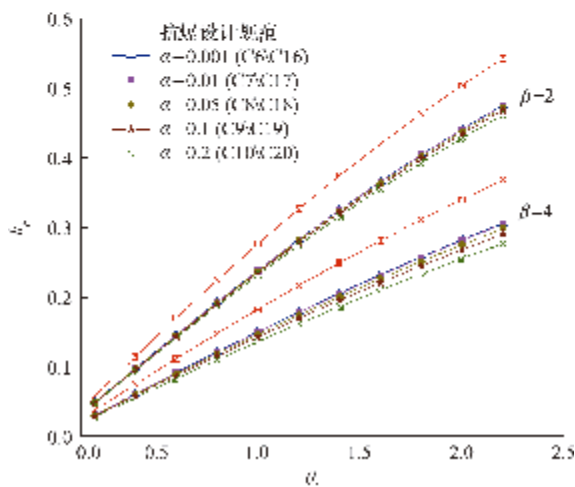
Tab. 2 Selection of typical calculation cases

工况	α	β	工况	α	β
C1	0.001	1.0	C11	0.001	3.0
C2	0.01	1.0	C12	0.01	3.0
C3	0.05	1.0	C13	0.05	3.0
C4	0.1	1.0	C14	0.1	3.0
C5	0.2	1.0	C15	0.2	3.0
C6	0.001	2.0	C16	0.001	4.0
C7	0.01	2.0	C17	0.01	4.0
C8	0.05	2.0	C18	0.05	4.0
C9	0.1	2.0	C19	0.1	4.0
C10	0.2	2.0	C20	0.2	4.0

注: α 和 β 分别代表抗力强化系数和延性比。



(a) $\beta=1$ 和 $\beta=3$ 时的动力系数曲线
(a) Dynamic coefficient curves for $\beta=1$ and $\beta=3$



(b) $\beta=2$ 和 $\beta=4$ 时的动力系数曲线
(b) Dynamic coefficient curves for $\beta=2$ and $\beta=4$

图 3 本文计算工况与规范公式结果对比

Fig. 3 Result comparison between calculation cases and code formula

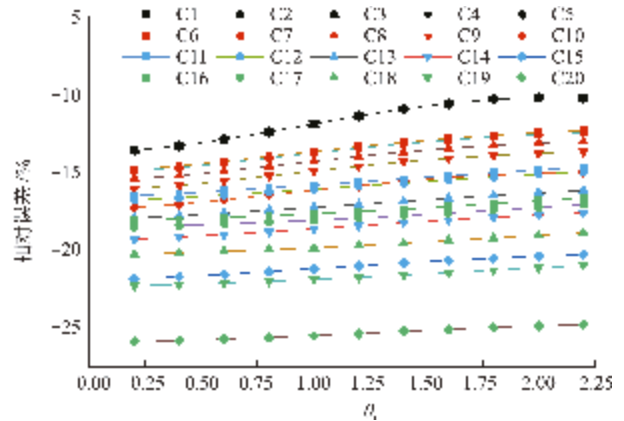


图 4 本文理论计算与规范公式的相对误差

Fig. 4 Relative error comparison between calculation cases and code formula

从图 3 和图 4 可以看出,柔性和刚性构件在不同延性比 β 工况下,均能光滑衔接;同一抗爆设计参数 θ_i 下,延性比 β 越大,即抗爆设计允许塑性变形越大,动力系数越低,抗爆设计等效静载越小,经济性越好;本文公式动力系数计算均小于抗爆设计规范计算值,延性比 $\beta=1.0$ 表示梁构件为弹性抗爆设计,无塑性变形,抗力强化系数 α 对动力系数的取值无影响,本文公式比规范公式低约 10.3%~13.6%,主要为考虑构件阻尼后产生的差异。延性比 $\beta=2\sim 4$ 时,抗力强化系数 $\alpha=0.001$ 和 0.01 对应的动力系数 k_d 差异性很小,约 0.1%~0.5%,这表明 $\alpha < 0.01$ 时,可忽略抗力强化效应,采用理想弹塑性抗力 SDOF 简化分析;抗力强化系数 $\alpha=0.05\sim 0.2$ 时较 $\alpha=0.001$ 对应的动力系数低约 0.7%~9.7%,且其数值低于规范值约 13.0%~25.9%,这表明采用塑性强化模型能有效降低抗爆设计荷载。

5 结论

本文理论推导了爆炸荷载作用下线性强化抗力模型梁构件的动力系数相关解析式,通过 DYNA 数值分析及规范对比工况算例,分析了含阻尼下塑性强化抗力参数对等效静载动力系数的影响,得到以下几点结论。

(1) 本文推导的动力系数解答在柔性和刚性两类构件衔接处光滑,计算结果与抗爆设计规范趋势相似,整体均低于抗爆设计规范,弹塑性抗爆构件随着抗力强化系数的增大,动力系数值逐渐降低。

(2) 当抗力强化系数小于 0.01 时,柔性和刚性两类构件计算出的动力系数与含阻尼理想弹性计算结果误差在 0.5%之内,此时可忽略抗力强

化系数影响,但忽略阻尼参数将带来较大误差。

(3) 当抗力强化系数为 0.05~0.2 时,其动力系数计算值与含阻尼理想弹塑性计算结果相对误差在 9.7% 之内,与现行国内抗爆设计规范相对差值在 10.3%~25.9%,此类参数下的梁构件类型宜考虑含阻尼的抗力强化模型。

参考文献(References):

- [1] 师燕超,张浩,李忠献. 钢筋混凝土梁式构件抗爆分析的改进等效单自由度方法[J]. 建筑结构学报, 2019, **40**(10): 8-16. (SHI Yan-chao, ZHANG Hao, LI Zhong-xian. Improved equivalent single degree of freedom method for blast analysis of RC beams[J]. *Journal of Building Structures*, 2019, **40**(10): 8-16. (in Chinese))
- [2] Biggs J M. *Introduction to Structural Dynamics* [M]. New York: McGraw-Hill Book Company, 1964.
- [3] 汤福静. 钢筋混凝土梁抗力函数的落锤实验研究[D]. 国防科学技术大学, 2011. (TANG Fu-jing. Experimental Study on Resistance Function of Reinforced Concrete Beams by Drop Hammer[D]. National University of Defense Technology, 2011. (in Chinese))
- [4] 张典典,于润清,张晓程. 基于能量的 RC 梁抗爆优化设计研究[J]. 建筑结构, 2016, **46**(S1): 696-701. (ZHANG Dian-dian, YU Run-qing, ZHANG Xiao-cheng. Energy based optimum blast resistant design and research for RC beam[J]. *Building Structure*, 2016, **46**(S1): 696-701. (in Chinese))
- [5] Jahami A, Temsah Y, Khatib J. The efficiency of using CFRP as a strengthening technique for reinforced concrete beams subjected to blast loading[J]. *International Journal of Advanced Structural Engineering*, 2019, **11**(4): 411-420.
- [6] GB 50009-2012. 建筑结构荷载规范[S]. 北京: 中国建筑工业出版社, 2012. (GB 50009-2012. Load Code for the Design of Building Structures [S]. Beijing: China Architecture & Building Press, 2012. (in Chinese))
- [7] CSA/S 850-12. Design and Assessment of Buildings Subjects to Blast Loads [S]. Canada: Canadian Standards Association, 2012.
- [8] 余俊,王海坤,刘建湖,等. 基于相变松弛法则的水下爆炸空化模型研究[J]. 计算力学学报, 2022, **39**(5): 684-690. (YU Jun, WANG Hai-kun, LIU Jian-Hu, et al. Research on cavitation model of underwater explosion based on phase transition relaxation algorithm [J]. *Chinese Journal of Computational Mechanics*, 2022, **39**(5): 684-690. (in Chinese))
- [9] 张传山,冯春,薛琨. 爆炸荷载下脆性颗粒体系破碎特性的数值研究[J]. 计算力学学报, 2022, **39**(3): 307-314. (ZHANG Chuan-shan, FENG Chun, XUE Kun. Numerical study on particle breakage characteristics under blast loading [J]. *Chinese Journal of Computational Mechanics*, 2022, **39**(3): 307-314. (in Chinese))
- [10] Liu Y, Yan J B, Huang F L. Behavior of reinforced concrete beams and columns subjected to blast loading[J]. *Defence Technology*, 2018, **14**(5): 550-559.
- [11] 陈万祥,郭志昆,罗立胜,等. 考虑面力效应的 HFR-LWC 梁抗爆理论模型与试验验证[J]. 工程力学, 2021, **38**(2): 77-91. (CHEN Wan-xiang, GUO Zhi-kun, LUO Li-sheng, et al. Theoretical model for HFR-LWC beam under blast loading accompanying membrane action and its experimental validation [J]. *Engineering Mechanics*, 2021, **38**(2): 77-91. (in Chinese))
- [12] Nagata M, Beppu M, Ichino H, et al. Method for evaluating the displacement response of RC beams subjected to close-in explosion using modified SDOF model [J]. *Engineering Structures*, 2018, **157**: 105-118.
- [13] Chen W X, Luo L S, Guo Z K, et al. Responses of HFR-LWC beams under close-range blast loadings accompanying membrane action[J]. *Defence Technology*, 2020, **16**(6): 1167-1187.
- [14] Yao S J, Zhang D, Lu F Y, et al. Damage features and dynamic response of RC beams under blast[J]. *Engineering Failure Analysis*, 2016, **62**: 103-111.
- [15] Wang W Y, Geng S B, Wang H, et al. Experimental study on the damage of steel tubular structural components by near-field detonations[J]. *KSCSE Journal of Civil Engineering*, 2021, **25**(2): 529-539.
- [16] Ritchie C B, Packer J A, Seica M V, et al. Behaviour and analysis of concrete-filled rectangular hollow sections subject to blast loading [J]. *Journal of Constructional Steel Research*, 2018, **147**: 340-359.
- [17] 方泰,杜茂林. 爆炸荷载作用下弹性与阻尼支承梁的动力响应[J]. 力学与实践, 2006, **28**(2): 53-56. (FANG Qin, DU Mao-lin. Dynamic responses of an elastically supported beams with damping subjected to blast loads[J]. *Mechanics in Engineering*, 2006, **28**(2): 53-56. (in Chinese))
- [18] 耿少波,罗干,陈佳龙,等. 阻尼对空爆荷载等效静载动力系数的影响[J]. 爆炸与冲击, 2022, **42**(2): 51-59. (GENG Shao-bo, LUO Gan, CHEN Jia-long, et al. Effect of damping on equivalent static load dynamic factor of air blast load [J]. *Explosion and Shock Waves*, 2022, **42**(2): 51-59. (in Chinese))
- [19] 蔡镇清,张昆,冉宪文,等. 基于 LS-DYNA 数值计

- 算和BP神经网络的钢筋混凝土构件抗力函数预测模型[J]. 机械设计, 2020, **37**(S2):1-9. (CAI Zhen-qing, ZHANG Kun, RAN Xian-wen, et al. Resistance function prediction model of reinforced concrete members based on LS-DYNA numerical calculation and BP neural network[J]. *Journal of Machine Design*, 2020, **37**(S2):1-9. (in Chinese))
- [20] Nassr A A, Yagi T, Maruyama T, et al. Damage and wave propagation characteristics in thin GFRP panels subjected to impact by steel balls at relatively low-velocities[J]. *International Journal of Impact Engineering*, 2018, **111**:21-33.
- [21] Bruhl J C, Varma A H. Analysis and design of one-way steel-plate composite walls for far-field blast effects[J]. *Journal of Structural Engineering*, 2021 (1):147.
- [22] Cui L L, Zhang X H, Hao H. Improved analysis method for structural members subjected to blast loads considering strain hardening and softening effects [J]. *Advances in Structural Engineering*, 2021, **24**(12):2622-2636.
- [23] GB 50038-2005. 人民防空地下室设计规范[S]. 北京: 中国计划出版社, 2006. (GB 50038-2005. Code for Design of Civil Air Defence Basement [S]. Beijing: China Planning Press, 2006. (in Chinese))
- [24] 方 泰, 柳锦春. 地下防护结构[M]. 北京: 中国水利水电出版社, 2010. (FANG Qin, LIU Jin-chun. *Underground Protective Structure* [M]. Beijing: China Water & Power Press, 2010. (in Chinese))

Study on dynamic coefficient of beam members with linear hardening resistance model under blast load

GENG Shao-bo^{1,2}, HAN Xiao-dan¹, NIU Yan-wei^{*2}, HAN Yun-shan¹, MA Lin-lin¹

(1. School of Environment and Safety Engineering, North University of China, Taiyuan 030051, China;

2. Research Center of Highway Large Structure Engineering on Safety, Ministry of Education, Chang'an University, Xi'an 710064, China)

Abstract: The ideal elastic-plastic resistance model is used extensively in the calculation of dynamic coefficients for beam members subjected to blast load. This conventional model restricts the refined analysis of blast resistant beam members with linear hardening resistance. In order to determine the dynamic coefficient of beam members with linear hardening resistance, according to the numerical relationship between resistance hardening coefficient and damping ratio, the analytical solutions of the dynamic coefficient based on the ductility ratio of flexible and rigid beam members are derived in three cases. The results of finite element analysis and specification comparison show that the derived theoretical formula has high accuracy and similar trend to the calculation results from blast resistant design specification formula. When the ductility ratio is 1, the hardening coefficient of resistance is independent of the dynamic coefficient. When the ductility ratio is greater than 1 and the hardening coefficient is less than 0.01, the influence of the hardening coefficient can be ignored. When the ductility ratio is greater than 2, the damping parameter should be considered in the beam blast resistant design analysis. When the ductility ratio is greater than 3 and the hardening coefficient is greater than 0.1, the linear hardening resistance model has better economic benefits.

Key words: linear hardening resistance model; blast load; dynamic coefficient; ductility ratio; beam member